GENERATION OF ATTOSECOND X-RAY PULSES WITH A MULTI-CYCLE TWO-COLOR ESASE SCHEME[*]

Y. Ding[†], Z. Huang, D. Ratner, SLAC, Menlo Park, CA 94025, USA

P. Bucksbaum, H. Merdji[‡], Stanford PULSE Center, SLAC, Menlo Park, CA 94025, USA

Abstract

Generation of attosecond x-ray pulses is attracting much attention within the x-ray free-electron laser (FEL) user community. Several schemes have been proposed based on manipulations of electron bunches with extremely short laser pulses. In this paper, we extend the attosecond two-color ESASE scheme proposed by Zholents *et al.* to the long optical cycle regime using a detuned second laser and a tapered undulator. Both lasers can be about ten-optical-cycles long, with the second laser frequency detuned from the first one to optimize the contrast between the central and side current spikes. A tapered undulator mitigates the degradation effect of the longitudinal space charge (LSC) force in the undulator and suppresses the FEL gain of all side current spikes. Simulations using the LCLS parameters show a single attosecond x-ray spike of ~ 110 attosecond can be produced with a good contrast ratio.

INTRODUCTION

Ultrashort soft and hard x-ray sources have the potential to open new regimes in atomic and electronic processes, benefiting widespread fields in physics, chemistry and biology. This has motivated the development of laser based ultrashort soft x-ray sources as well as the construction of fourth generation free electron laser (FEL) sources in the soft and hard x-ray regime. Due to the duration of the electron bunch, FEL facilities have aimed for the femtosecond regime, but the formidable challenge of generating attosecond pulses is attracting much attention within the x-ray FEL user community. Several schemes for generation of attosecond x-ray pulses have been proposed [1, 2, 3, 4, 5, 6, 7, 8], mostly based on manipulations of electron bunches with extremely short laser pulses.

The two-color scheme proposed in Ref. [6] is based on the current-enhanced self-amplified spontaneous emission (ESASE) technique proposed by Zholents [9]. The electron beam experiences an energy modulation upon interacting with two laser pulses within two single-period wiggler magnets. Each laser interacts with the same group of electrons at its focal point in the center of the wigglers. A dispersive section, such as a four-dipole chicane, converts the energy modulation of the electron bunch to the density modulation. The high-current spike formed by the overlapping peak intensities of the two lasers dominates the FEL gain process and produces an attosecond x-ray pulse. Ultra-short lasers with no more than two optical cycles are required to minimize satellite spikes. In addition, longitudinal space charge effects in the main FEL undulator have to be considered properly [10].

In this paper, we extend the attosecond two-color ESASE scheme to the long optical cycle regime using a detuned second laser and a tapered undulator. Our scheme extends to FELs a technique proposed for high-order harmonic generation (HHG) to manipulate an electron wave packet for the generation of isolated attosecond soft X-ray pulses [11]. HHG experiments have shown a controlled detuning between the two colors can control the electron wave packet energy (low energy regime) in the sub-cycle domain using relatively long infrared laser pulses (up to 15 optical cycles). Here, we apply this idea to ESASE. Both lasers can be about ten optical cycles long, with the second laser frequency detuned from the first one to optimize the contrast between the central and side current spikes. A tapered undulator mitigates the degradation effect of the LSC force in the undulator [10] and suppresses the FEL gain of all side current spikes. Our proposal extends the original proposal of Zholents *et al.* to relatively long commercially available infrared laser pulses, making a more reliable and user-friendly attosecond X-ray FEL.

OPTIMIZATION OF THE ENERGY MODULATION

We use similar parameters as in Ref. [6] but with relatively long laser pulses of about 10 optical cycles or more. A schematic setup is shown in Fig. 1. Table 1 summarizes the main parameters for electron beam, lasers and wigglers used in this paper. The electron beam in this study is based on the standard Linac Coherent Light Source (LCLS) setup, i.e., the beam current is 3.4 kA, the electron energy is 13.6 GeV, the normalized emittance is 1.2 μm, and the energy spread is 1.1 MeV. A laser system to generate a tunable sub-harmonic field is described in ref. [14] with the use of optical parametric amplification. Here the fundamental laser (we call it laser-1) has a wavelength of 0.8 μm with a pulse length of 25 fs (FWHM of intensity). Laser-1 is focused at the center of the first wiggler (W1), with carrier wave phase adjusted to be zero-crossing at the peak of the laser envelope. After interaction in W1 with a laser power of 20 GW the electrons have an energy modulation amplitude of 3.8 MeV at the center of the bunch.

We optimize the energy modulation by tuning the second
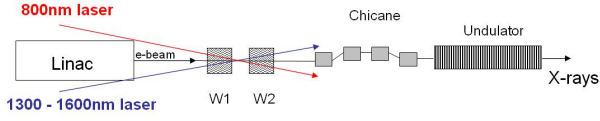
Figure 1: (color) Schematic setup for the two-color ESASE.

Figure 2: (color) Calculated longitudinal phase space of the electrons after interaction with two lasers.

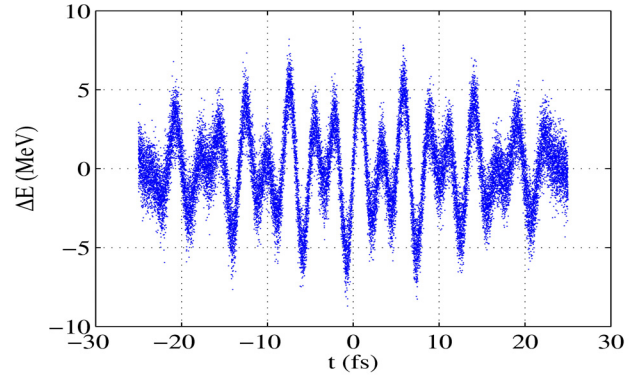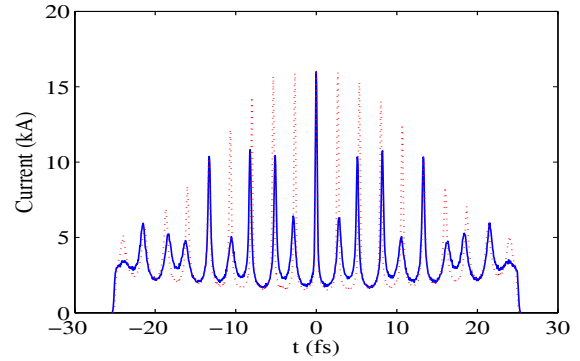Figure 3: (color) Current profile after a bunching chicane. Solid blue curve is from two optimized lasers, while red dotted curve is from laser-1 only.

laser (laser-2) frequency, intensity and pulse length. The wavelength of laser-2 is optimized to be 1.314 μm with a pulse length of 45 fs (FWHM of intensity). To make an effective energy modulation, laser-2 interacts at the center of the second wiggler (W2) with the same group of the electrons, also at a zero-crossing phase. After interacting in W2, the electrons gain an additional energy modulation of 1.7 MeV at the bunch center when using a power of 2.4 GW from laser-2. Fig. 2 shows the combined energy modulation of the electrons after interacting with the two lasers. The total energy modulation amplitude at the center of the bunch is 5.5 MeV. The resulting current profile after a full compression on the central period of the energy-modulated bunch is shown in Fig. 3 with solid blue curve. A current profile with laser-1 only (increased laser power) is also shown in the figure with a dotted red curve. The contrast ratio obtained between the central peak and side maximum peak using an optimized detuning laser is about 17kA/11kA, much better than from the single laser case.

Table 1: Main parameters for electrons,lasers and wigglers

	parameter	value	unit
Electron	Energy	13.6	GeV
	peak current	3.4	kA
	rms emittance	1.2	μm
	rms energy spread	1.1	MeV
Laser-1	wavelength	0.8	μm
	power	20	GW
	FWHM of intensity	25	fs
Laser-2	wavelength	1.314	μm
	power	2.4	GW
	FWHM of intensity	45	fs
Wiggler-1	period	0.5	m
	wiggler parameter K_{w1}	67.3	
Wiggler-2	period	0.5	m
	wiggler parameter K_{w2}	86.3	
Undulator	period	3	cm
	undulator parameter K	3.5	
	average beta function	18	m

LONGITUDINAL SPACE CHARGE IN THE FEL UNDULATOR

After the bunching chicane, the energy modulation is converted to a density modulation and the peak current of the central spike can reach 17 kA in our case, as shown in Fig. 3. Since only a small section of the bunch charge is concentrated in the spike region, the emittance growth due to coherent synchrotron radiation in the chicane and transverse space charge in the main undulator is negligible. However, due to the wiggling motion in the undulator, the longitudinal space charge field is equivalent to the free space result by changing γ to $\bar{\gamma}_z$, where $\bar{\gamma}_z = \gamma/\sqrt{1 + K^2/2}$, and K is the undulator parameter [10]. In the limit when the electron bunch length in the average co-moving frame is much larger than the transverse beam size, we can use a simplified expression to estimate the longitudinal space charge field [12]:

$$E_z \approx -\frac{Z_0 I'(s)}{4\pi\bar{\gamma}_z^2}\left(2\ln\frac{\bar{\gamma}_z\sigma_z}{r_b} + 1 - \frac{r^2}{r_b^2}\right), \qquad (1)$$

where $r = \sqrt{x^2 + y^2}$, $Z_0 = 377$ Ω, $I'(s) = dI/ds$ is the derivative of the electron current profile with respect to the bunch longitudinal coordinate s, σ_z is the rms bunch length, and r_b is the beam radius of a uniform transverse distribution. Here we take $\bar{\gamma}_z \sim 10000$, $r_b \approx 2\sigma_x \sim 60$ μm, and central spike $\sigma_z \sim 40$ nm. With these parameters, E_z depends very weakly on the transverse position of the electron within the beam. Hence we will drop the r-dependent term in computing the LSC field.

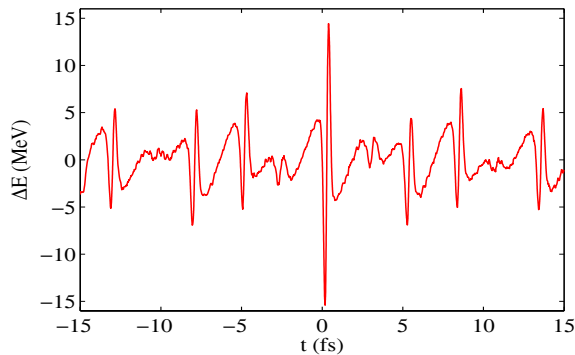Figure 4 shows the accumulated energy spread due to the

X-ray FELs

Figure 4: (color) Electron bunch energy variation from the LSC field after a distance of 50 m in the LCLS undulator (head of the bunch is to the right).
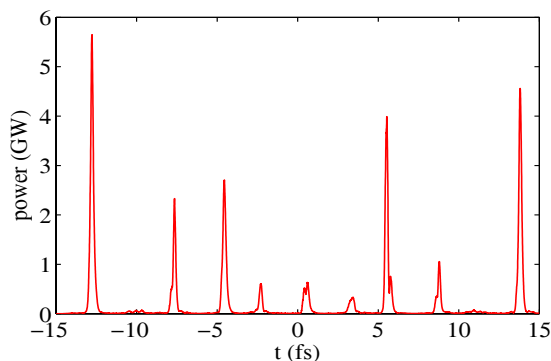

Figure 5: (color) A typical example of the radiation profile at the undulator distance of 50 m without any undulator tapering.

LSC effect at a distance of 50 m in the undulator. For the central current spike, LSC produces a strong energy chirp with a peak-to-peak energy variation of about 30 MeV. Such a large energy spread can degrade the FEL interaction because it is larger than the FEL bandwidth. We include this LSC effect in *GENESIS* [13] simulations. A typical radiation profile at 50 m is shown in Fig. 5, where the normal undulator parameters of LCLS were used, i.e., $\lambda_u = 3$ cm, $K = 3.5$ and average beta function in the undulator of 18 m. By creating a large energy chirp, the LSC force effectively suppresses radiation from the central spike.

TAPERED UNDULATORS

A tapered undulator can prevent FEL gain degradation in a linearly chirped electron beam [7]. The resonant FEL radiation wavelength is a function of electron energy, which can change along the undulator. Compared with the scheme in [7] where a fixed energy chirp is formed before electrons entering the undulator, an energy chirp due to LSC grows linearly in the undulator. As the electrons move along the undulator, the LSC fields produce an energy chirp that shifts the electrons away from their original resonant

wavelength, changing the resonant condition and suppressing the FEL process. By tapering the undulator parameter, K, we can compensate for the energy change, and preserve the resonant condition. However, because the strength of the LSC fields depends on the derivative of the current, the proper taper strength will be larger for the central spikes than for the side spikes. In our scheme, we detuned the second laser frequency to obtain the best contrast ratio between the central and side current peaks. We can see from Fig. 4 that the energy modulation of the central peak is about a factor of 2 larger than for the side peaks. By choosing the taper to match the chirp of the central spike, where the energy chirp is strongest, we can preserve the resonant condition in this region, while simultaneously suppressing the FEL process elsewhere in the bunch. At the same time, the larger current at the central peak also helps to obtain a higher FEL gain than at the side peaks. The combination of current and taper effects provide a good contrast ratio between the central and side x-ray spikes.

We used *GENESIS* code to optimize the undulator taper. Tapers used to compensate for energy loss from radiation require K to decrease along the undulator; in contrast, here we require a taper with K increasing (defined as a negative taper in [7]) to offset the LSC-induced energy increase in the head part of the central spike. Fig. 6 shows the x-ray power profile using a negative taper of 1% from 15 m to 70 m. The result in this figure is averaged over 10 shot noise realizations because of large statistical fluctuations on each spike. A nice contrast ratio over a factor of 10 is obtained between the central and side spikes. The FWHM of the central spike is about 110 attosecond with an averaged peak power about 2 GW at 50 m undulator length. Compared to the normal LCLS configuration with a more uniform electron bunch current, the two-color ESASE discussed here shows strong FEL slippage effects in the narrow current spike region. As a result, the x-ray pulse duration obtained here is shorter than the typical SASE spike duration of 300 as in the standard LCLS configuration, but the saturated FEL power is also reduced.

COHERENT CONTROL ON THE X-RAY RADIATION PULSE

The second laser wavelength is optimized to be 1.314 μm to obtain a single spike x-ray pulse (single mode). From laser technique, this laser could be tunable between 1.3 to 2 μm [14]. Tuning only the wavelength of laser-2 changes the contrast ratio between the central and side spikes in the current profile, hence the x-ray radiation pulse length can be coherently controlled. The taper of the main undulator is fixed at the optimized value to generate a single attosecond pulse, and the laser-2 wavelength is tuned from 1.6 μm down to 1.3 μm. We performed simulations at laser-2 wavelength of 1.6 μm and 1.45 μm. Fig. 7 shows the current profiles and corresponding radiation pulses at the two modes. At a wavelength of 1.6 μm for laser-2, all but four of the side peaks are suppressed. More suppres-
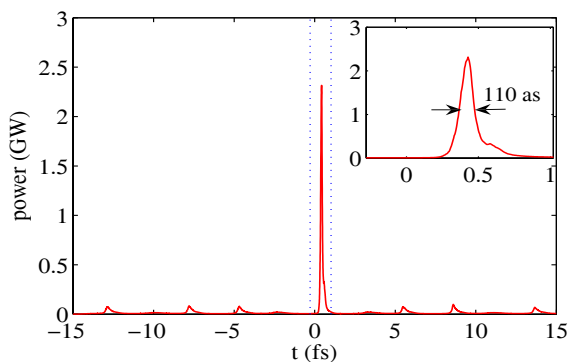
Figure 6: (color) X-ray power profile (averaged over 10 shot noise realizations) at the undulator length of 50 m with an optimized undulator tapering of 1% from 15 m to 50 m. The inset zooms to the central spike in the dotted blue region.
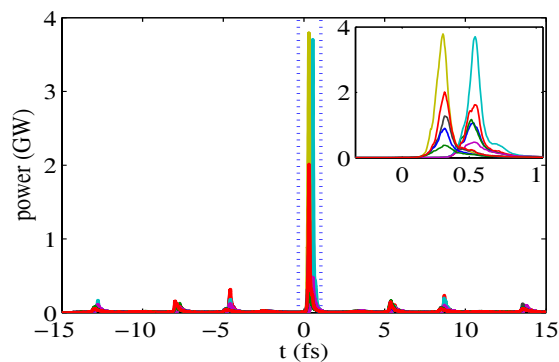

Figure 8: (color) Radiation profiles with a phase shift of 0.1fs and -0.1fs between the two lasers, five runs for each phase shift using diffrent shot noise realizaitons. The inset zooms to the central spikes in the dotted blue region.
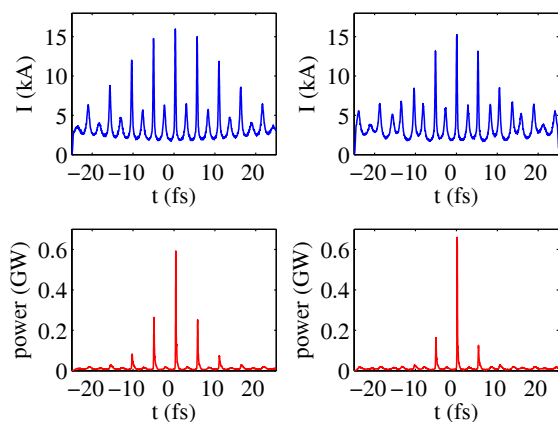
central spike and side ones is also reduced. It should be noted that interferometric stability is intrinsically achieved in the optical parametric amplifier set-up. Mechanical instabilities are usually circumvented using stable table-top laser set-up combined with active adaptive optics.

Figure 7: (color) Current profiles and radiation pulses vs. detuning of the second laser. Left: laser-2 wavelength of 1.6 μm; Right: laser-2 wavelength of 1.45 μm.

sion of side spikes continues when tuning laser-2 to 1.45 μm until arriving at the single spike mode described at last section.

DISCUSSIONS

In this paper, we discussed an improved method of two-color ESASE to obtain a single attosecond pulse with an optimized undulator taper. By changing the second laser wavelength, we can coherently control the x-ray radiation duration from attosecond to femtosecond regimes.

The relative shift between the carrier envelope phases of the two lasers is a critical issue in this scheme. Figure 8 shows an example of the radiation profiles assuming a phase shift of ± 0.1 fs between two lasers, with five runs for each phase shift value using different shot noise realizations. Compared with Fig 6, the central spike locations change about $\pm 0.1 fs$, and the contrast ratio between the

X-ray FELs

REFERENCES

[1] E.L. Saldin, E.A. Schneidmiller, and M.V. Yurkov, Opt. Commun. **212**, 377 (2002).

[2] A. A. Zholents and W. M. Fwaley, Phys. Rev. Lett. **92**, 224801 (2004).

[3] E.L. Saldin, E.A. Schneidmiller, and M.V. Yurkov, Opt. Commun. **237**,153 (2004).

[4] E.L. Saldin, E.A. Schneidmiller, and M.V. Yurkov, Opt. Commun. **239**,161 (2004).

[5] P. Emma, Z. Huang, M. Borland, in Proceedings of FEL2004 (Trieste, Italy, 2004).

[6] A. A. Zholents and G. Penn, Phys. Rev. ST-AB **8**, 050704 (2005).

[7] E.L. Saldin, E.A. Schneidmiller, and M.V. Yurkov, Phys. Rev. ST-AB **9**, 050702 (2006).

[8] A. A. Zholents and M S Zolotorev, New J. Phys. **10**, 025005 (2008).

[9] A. A. Zholents, Phys. Rev. ST-AB **8**, 040701 (2005)

[10] G. Geloni *et al.*, Nucl. Instrum. Methods A **583**, 228 (2007)

[11] H. Merdji *et al.*, Opt. Lett. **32** 3134 (2007).

[12] A. W. Chao, *Physics of collective beam instabilities in high energy accelerators* (John Wiley & Sons, 1993).

[13] S. Reiche, Nucl. Instrum. Methods **A** 429, 243 (1999).

[14] C. Vozzi *et al.*, Opt. Lett. **32** 2957 (2007).